CHAPTER – 5

AN EXPERIMENTAL AND THEORETICAL APPROACH ON THE MOLECULAR STRUCTURE AND EFFECT OF HYDROGEN BONDING IN THE VIBRATIONAL SPECTRA OF SULFASALAZINE, AN ANTIBACTERIAL DRUG

Sulfonamide compounds competing with p-aminobenzoic acid inhibits the bacterial enzyme dihydropteroate synthetase which is required by bacteria for the synthesis of folic acid, a compound essential for bacterial growth [23]. The compound 5-{4-[(2-pyridylamino)sulfonyl]phenyldiazenyl}salicylic acid under study is commonly known as sulfasalazine is an antibacterial sulfonamide compound. This compound is a diazo link of sulfapyridine with a 5-aminosalicylic acid (5-ASA). Sulfapyridine is an antibacterial agent and 5-ASA is an anti-inflammatory agent. The efficacy of sulfasalazine in inflammatory bowel disease (IBD) and rheumatoid arthritis is well established [106-108]. Sulfasalazine is widely used in women of reproductive age with IBD because it is effective, cheap and safe during pregnancy and lactation [109]. Sulfasalazine releases sulfapyridine and 5-ASA in the colon and enables their application for intestinal infections like ulcerative colitis [110]. The antibacterial effect of sulfasalazine has decreased the number of anaerobic bacteria in the faecal flora of patients with IBD [111]. Also sulfasalazine obstructs the growth of tactile allodynia in diabetes rats. This justifies the studies to test the effects of sulfasalazine on altered nociception in diabetic patients [112]. Sulfasalazine becomes an alternative therapy in some patients with moderate to severe psoriasis [113]. In the crystalline state, two sulfasalazine molecules form a centrosymmetric dimer by the intermolecular N–H···O and O–H···N hydrogen bonds and the compound is more stabilized by the intramolecular O–H···O interaction [114].

Spectroscopic and density functional theory studies on various sulfonamide compounds have been reported [115-117]. The complexes of sulfasalazine with some alkaline metals Mg(II), Ca(II), Sr(II) and Ba(II) have been investigated [118]. Characterization of the ternary complexes of nickel with sulfasalazine and some amino acids based on elemental analysis, IR, UV-vis, mass spectra and thermal analysis have been reported [119]. The charge transfer interactions between the antibiotic drug sulfasalazine and the acceptors picric acid, iodine etc. have been studied spectrophotometrically in chloroform or methanol solutions [26]. The structures of Cerium(IV), Thorium(IV) and Uranyl(II) complexes with the ammonium salt of sulfasalazine drug have been studied using elemental analysis, IR, mass spectroscopy and thermal analysis [120]. In the present work, the molecular modeling of sulfasalazine monomer and dimer has been done in the B3LYP density functional, using 6-311G (d, p) basis set. The intramolecular and intermolecular hydrogen bonding interactions have been investigated using natural bond orbital (NBO) analysis. Vibrational assignments of sulfasalazine monomer have been performed using the scaled quantum mechanical force field technique and effect of hydrogen bonding in the spectra is observed.

5.1 Experimental details

The title compound sulfasalazine of 98% purity was purchased from Sigma-Aldrich and used without further purification. The Fourier-transform infrared spectrum of sulfasalazine is recorded in the region 4000 – 450 cm^{-1} with the Perkin-Elmer Spectrum One FT-IR spectrometer using KBr pellet technique. The resolution of the spectrum is 1 cm^{-1}. The Fourier-transform Raman spectrum of resolution 2 cm^{-1} is recorded using Bruker RFS 27 Stand alone FT-Raman spectrometer in the

spectral range 4000 – 50 cm^{-1}. Nd: YAG laser at 1064 nm is used as the exciting source.

5.2 Optimized geometries

The optimized molecular structure with the numbering scheme of sulfasalazine monomer is presented in Fig. 5.1. The calculated geometry of sulfasalazine monomer and dimer in B3LYP/6-311G (d, p) level with the experimental [114] data are given in Tables 5.1, 5.2 and 5.3.

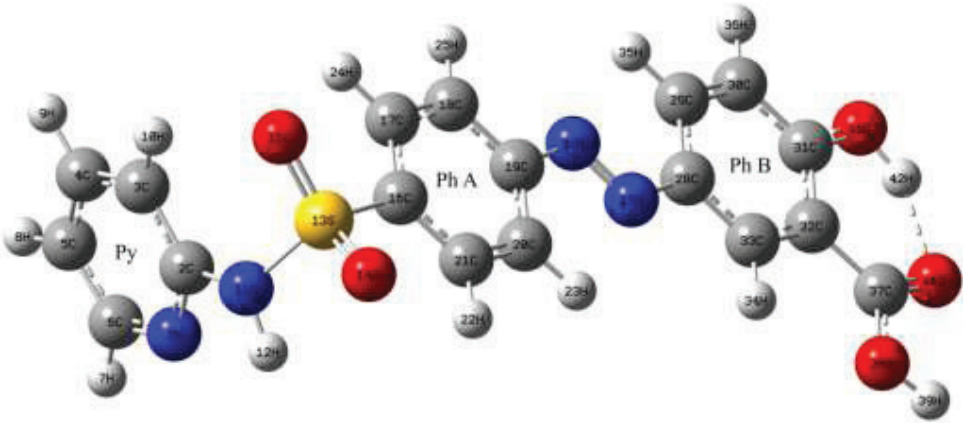

Fig. 5.1 Optimized molecular structure and atomic numbering of sulfasalazine monomer.

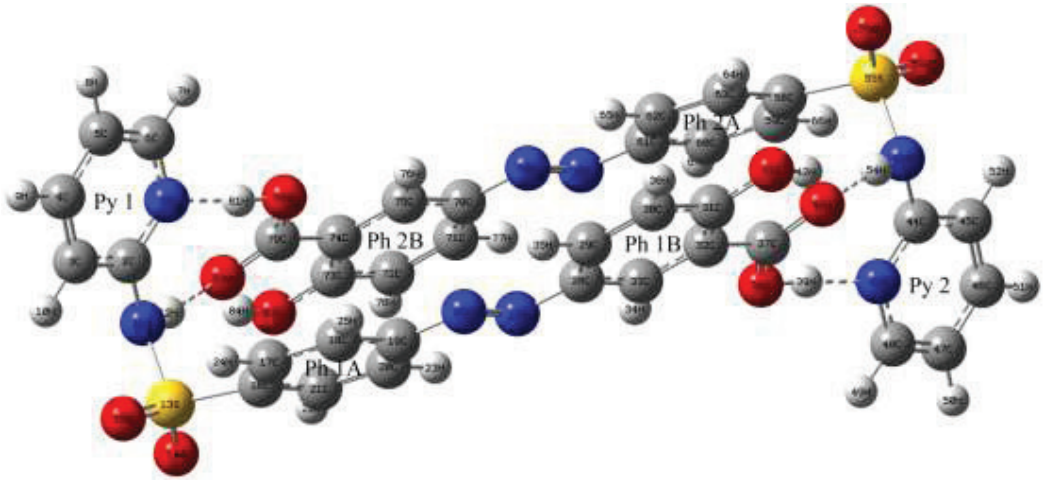

Fig. 5.2 Optimized molecular structure and atomic numbering of sulfasalazine dimer.

Two sulfasalazine molecules form a centrosymmetric dimer by the intermolecular hydrogen bonds N–H···O and O–H···N. The optimized structure of sulfasalazine with the N_{11}–H_{12}···O_{82}, O_{38}–H_{39}···N_{43} and N_{53}–H_{54}···O_{40}, O_{80}–H_{81}···N_1 interaction forming the dimer structure is shown in Fig. 5.2 and the hydrogen bond geometry is given in Table 5.4. The bridging part (intra and intermolecular hydrogen bonding) of sulfasalazine dimer in shown in Fig. 5.3. The calculated geometry of the molecule agrees well with the experimental data except some deviation in the isolated molecule due to the ignorance of hydrogen bonded interaction. The bond lengths N_{11}–H_{12} and N_{11}–S_{13} increases (~0.01Å) upon dimerization. The length of O_{38}–H_{39} bond is elongated to large extent (0.05 Å) upon dimerization due to strong O_{38}–H_{39}···N_{43} intermolecular interaction. The bond length C_{37}−O_{38} decreases by 0.03Å and C_{37}−O_{40} increases by 0.01Å due to redistribution of charges. The D···A distance of O_{38}–H_{39}···N_{43} in dimer is 2.692Å, shorter than the van der Waals radii 2.750Å showing the strength of hydrogen bond [121].

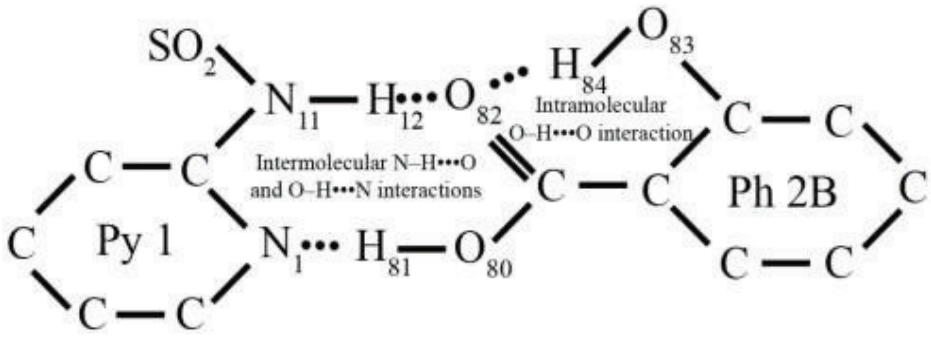

Fig. 5.3 Bridging part (intra and intermolecular hydrogen bonding) of sulfasalazine dimer.

Table 5.1 Bond lengths of sulfasalazine monomer and dimer by B3LYP/ 6-311G (d,p) in comparison with the XRD data.

Bond length	Calc. (Å)		Expt. [114] (Å)
	Monomer	Dimer	
N_1–C_2	1.334	1.342	1.340
N_1–C_6	1.336	1.342	1.338
C_2–C_3	1.401	1.401	1.373
C_2–N_{11}	1.413	1.405	1.425
C_3–C_4	1.388	1.386	1.381
C_3–H_{10}	1.081	1.080	0.930
C_4–C_5	1.394	1.396	1.371
C_4–H_9	1.084	1.084	0.929
C_5–C_6	1.390	1.385	1.370
C_5–H_8	1.083	1.082	0.930
C_6–H_7	1.086	1.085	0.930
N_{11}–H_{12}	1.015	1.026	0.993
N_{11}–S_{13}	1.691	1.701	1.654
S_{13}–O_{14}	1.454	1.453	1.426
S_{13}–O_{15}	1.456	1.457	1.426
S_{13}–C_{16}	1.797	1.796	1.764
C_{16}–C_{17}	1.392	1.393	1.379
C_{16}–C_{21}	1.399	1.399	1.392
C_{17}–C_{18}	1.391	1.390	1.380
C_{17}–H_{24}	1.082	1.082	0.930
C_{18}–C_{19}	1.398	1.399	1.381
C_{18}–H_{25}	1.083	1.083	0.930
C_{19}–C_{20}	1.404	1.404	1.384
C_{19}–N_{26}	1.418	1.417	1.427
C_{20}–C_{21}	1.384	1.385	1.377
C_{20}–H_{23}	1.081	1.081	0.930
C_{21}–H_{22}	1.083	1.083	0.930
N_{26}–N_{27}	1.256	1.257	1.249
N_{27}–C_{28}	1.407	1.405	1.426
C_{28}–C_{29}	1.413	1.414	1.403
C_{28}–C_{33}	1.390	1.391	1.373

Bond length	Calc. (Å)		Expt. [114] (Å)
	Monomer	Dimer	
C_{29}–C_{30}	1.375	1.375	1.362
C_{29}–H_{35}	1.082	1.082	0.930
C_{30}–C_{31}	1.409	1.410	1.393
C_{30}–H_{36}	1.083	1.083	0.930
C_{31}–C_{32}	1.419	1.419	1.399
C_{31}–O_{41}	1.333	1.333	1.345
C_{32}–C_{33}	1.400	1.399	1.398
C_{32}–C_{37}	1.467	1.473	1.471
C_{33}–H_{34}	1.082	1.082	0.930
C_{37}–O_{38}	1.343	1.313	1.294
C_{37}–O_{40}	1.225	1.242	1.239
O_{38}–H_{39}	0.969	1.019	1.005
O_{41}–H_{42}	0.984	0.986	0.910

The bond angles associated with the pyridine ring C_2–N_1–C_6, N_1–C_2–C_3, N_1–C_2–N_{11} and C_3–C_2–N_{11} are tilted up to 1.05°, 1.55°, 2.69°, 1.14° respectively due to the involvement of the pyridine ring in the hydrogen bonding. The N_{11}–H_{12}···O_{82} hydrogen bonding distorts the bond angles C_2–N_{11}–H_{12} and C_2–N_{11}–S_{13} upto 2.38° and 3.61° respectively. The deviation of 2.51° in the bond angle C_{32}–C_{37}–O_{40} of monomer to dimer species is due to the hydrogen bonding. The apparent difference (8.04°) noticed in the intramolecular O_{41}–H_{42}···O_{40} bond angle (Table 5.4) between experimental and computational value is due to non-consideration of the short contact interaction with neighboring molecules in computation. The planarity of the pyridine ring and the phenyl rings (Ph A and Ph B) are known from the dihedral angles (Table 5.3). The dihedral angles C_{18}–C_{19}–N_{26}–N_{27}, C_{20}–C_{19}–N_{26}–N_{27}, C_{19}–N_{26}–N_{27}–C28, N_{26}–N_{27}–C_{28}–C_{29} and N_{26}–N_{27}–C_{28}–C_{33} show that the phenyl rings A and B are coplanar whereas the Py ring is inclined (~-31.18°) to the phenyl ring.

Table 5.2 Bond angles of sulfasalazine monomer and dimer by B3LYP/6-311G (d, p) in comparison with the XRD data.

Bond angle	Calc. (°)		Expt. [114] (°)
	Monomer	Dimer	
C_2–N_1–C_6	117.85	118.90	117.93
N_1–C_2–C_3	123.59	122.04	122.49
N_1–C_2–N_{11}	113.61	116.30	115.73
C_3–C_2–N_{11}	122.74	121.60	121.77
C_2–C_3–C_4	117.46	118.34	118.38
C_2–C_3–H_{10}	120.40	119.46	120.82
C_4–C_3–H_{10}	122.13	122.20	120.80
C_3–C_4–C_5	119.76	119.73	119.78
C_3–C_4–H_9	119.70	119.80	120.10
C_5–C_4–H_9	120.53	120.46	120.12
C_4–C_5–C_6	117.86	117.99	118.23
C_4–C_5–H_8	121.55	121.61	120.91
C_6–C_5–H_8	120.58	120.40	120.86
N_1–C_6–C_5	123.47	122.96	123.13
N_1–C_6–H_7	115.72	115.80	118.39
C_5–C_6–H_7	120.81	121.24	118.48
C_2–N_{11}–H_{12}	111.79	114.17	112.46
C_2–N_{11}–S_{13}	126.15	122.54	117.49
H_{12}–N_{11}–S_{13}	111.91	111.95	109.47
N_{11}–S_{13}–O_{14}	103.93	104.68	105.23
N_{11}–S_{13}–O_{15}	107.30	107.00	107.44
N_{11}–S_{13}–C_{16}	105.94	104.02	104.87
O_{14}–S_{13}–O_{15}	122.73	122.75	120.15
O_{14}–S_{13}–C_{16}	108.14	108.79	109.46
O_{15}–S_{13}–C_{16}	107.66	108.04	108.60
S_{13}–C_{16}–C_{17}	119.62	119.34	118.64
S_{13}–C_{16}–C_{21}	118.96	119.04	120.31
C_{17}–C_{16}–C_{21}	121.42	121.43	120.76
C_{16}–C_{17}–C_{18}	118.82	118.81	119.07
C_{16}–C_{17}–H_{24}	120.05	120.04	120.50
C_{18}–C_{17}–H_{24}	121.12	121.15	120.44
C_{17}–C_{18}–C_{19}	120.51	120.54	120.63
C_{17}–C_{18}–H_{25}	121.10	121.10	119.74
C_{19}–C_{18}–H_{25}	118.39	118.35	119.64

Bond angle	Calc. (°)		Expt. [114] (°)
	Monomer	Dimer	
C_{18}–C_{19}–C_{20}	119.94	119.86	120.05
C_{18}–C_{19}–N_{26}	115.54	115.51	114.60
C_{20}–C_{19}–N_{26}	124.52	124.59	125.35
C_{19}–C_{20}–C_{21}	119.90	119.95	119.85
C_{19}–C_{20}–H_{23}	118.95	118.90	120.07
C_{21}–C_{20}–H_{23}	121.16	121.14	120.08
C_{16}–C_{21}–C_{20}	119.42	119.36	119.62
C_{16}–C_{21}–H_{22}	119.91	119.79	120.22
C_{20}–C_{21}–H_{22}	120.65	120.85	120.16
C_{19}–N_{26}–N_{27}	114.74	114.78	115.05
N_{26}–N_{27}–C_{28}	115.43	115.45	113.38
N_{27}–C_{28}–C_{29}	124.78	124.65	123.59
N_{27}–C_{28}–C_{33}	115.98	116.09	117.16
C_{29}–C_{28}–C_{33}	119.25	119.21	119.24
C_{28}–C_{29}–C_{30}	120.59	120.53	120.53
C_{28}–C_{29}–H_{35}	118.44	118.48	119.72
C_{30}–C_{29}–H_{35}	120.97	120.99	119.75
C_{29}–C_{30}–C_{31}	120.58	120.61	120.43
C_{29}–C_{30}–H_{36}	121.60	121.62	119.76
C_{31}–C_{30}–H_{36}	117.81	117.76	119.81
C_{30}–C_{31}–C_{32}	119.22	119.26	119.95
C_{30}–C_{31}–O_{41}	117.80	117.67	117.59
C_{32}–C_{31}–O_{41}	122.98	123.06	122.45
C_{31}–C_{32}–C_{33}	119.34	119.22	118.66
C_{31}–C_{32}–C_{37}	118.68	119.40	120.30
C_{33}–C_{32}–C_{37}	121.98	121.36	121.03
C_{28}–C_{33}–C_{32}	121.02	121.12	121.16
C_{28}–C_{33}–H_{34}	118.88	119.08	119.46
C_{32}–C_{33}–H_{34}	120.09	119.79	119.39
C_{32}–C_{37}–O_{38}	114.67	115.94	115.26
C_{32}–C_{37}–O_{40}	124.10	121.59	121.97
O_{38}–C_{37}–O_{40}	121.23	122.47	122.77
C_{37}–O_{38}–H_{39}	106.78	110.43	112.74
C_{31}–O_{41}–H_{42}	107.71	107.42	102.88

Table 5.3 Dihedral angles of sulfasalazine monomer and dimer by B3LYP/6-311G (d, p) in comparison with the XRD data.

Dihedral angle	Calc. (°)		Expt. [114] (°)
	Monomer	Dimer	
$C_6–N_1–C_2–C_3$	-0.05	-1.42	1.02
$C_6–N_1–C_2–N_{11}$	177.04	175.98	179.80
$C_2–N_1–C_6–C_5$	1.34	2.03	1.13
$C_2–N_1–C_6–C_7$	-179.13	-178.84	-178.90
$N_1–C_2–C_3–C_4$	-1.17	-0.29	-2.30
$N_1–C_2–C_3–H_{10}$	177.64	179.40	177.63
$N_{11}–C_2–C_3–C_4$	-178.00	-177.56	178.56
$N_{11}–C_2–C_3–H_{10}$	0.82	2.13	-1.50
$N_1–C_2–N_{11}–H_{12}$	-1.98	-17.38	-21.36
$N_1–C_2–N_{11}–S_{13}$	140.19	123.18	107.09
$C_3–C_2–N_{11}–H_{12}$	175.14	160.03	157.83
$C_3–C_2–N_{11}–S_{13}$	-42.70	-59.40	-73.73
$C_2–C_3–C_4–C_5$	1.14	1.43	1.49
$C_2–C_3–C_4–H_9$	-179.9	-179.95	-178.49
$H_{10}–C_3–C_4–C_5$	-177.65	-178.25	-178.45
$H_{10}–C_3–C_4–H_9$	1.30	0.37	1.58
$C_3–C_4–C_5–C_6$	0.01	-0.88	0.49
$C_3–C_4–C_5–H_8$	179.42	178.94	-179.53
$H_9–C_4–C_5–C_6$	-178.93	-179.48	-179.54
$H_9–C_4–C_5–H_8$	0.48	0.33	0.45
$C_4–C_5–C_6–N_1$	-1.32	-0.89	-1.87
$C_4–C_5–C_6–H_7$	179.17	-179.97	178.16
$H_8–C_5–C_6–N_1$	179.26	179.29	178.15
$H_8–C_5–C_6–H_7$	-0.25	0.21	-1.83
$C_2–N_{11}–S_{13}–O_{14}$	-177.67	178.20	-176.44
$C_2–N_{11}–S_{13}–O_{15}$	50.98	46.53	54.42
$C_2–N_{11}–S_{13}–C_{16}$	-63.82	-67.68	-61.00
$H_{12}–N_{11}–S_{13}–O_{14}$	-35.54	-40.47	-46.59
$H_{12}–N_{11}–S_{13}–O_{15}$	-166.90	-172.14	-175.73
$H_{12}–N_{11}–S_{13}–C_{16}$	78.31	73.65	68.85
$N_{11}–S_{13}–C_{16}–C_{17}$	97.85	91.86	86.36
$N_{11}–S_{13}–C_{16}–C_{21}$	-81.26	-83.23	-87.50
$O_{14}–S_{13}–C_{16}–C_{17}$	-151.24	-156.98	-161.18
$O_{14}–S_{13}–C_{16}–C_{21}$	29.65	27.92	24.96
$O_{15}–S_{13}–C_{16}–C_{17}$	-16.70	-21.60	-28.26
$O_{15}–S_{13}–C_{16}–C_{21}$	164.19	163.30	157.88
$S_{13}–C_{16}–C_{17}–C_{18}$	-178.74	-173.21	-173.41
$S_{13}–C_{16}–C_{17}–H_{24}$	2.64	6.98	6.64
$C_{21}–C_{16}–C_{17}–C_{18}$	0.35	1.77	0.43

Dihedral angle	Calc. (°)		Expt. [114] (°)
	Monomer	Dimer	
C_{21}–C_{16}–C_{17}–H_{24}	-178.27	-178.04	-179.52
S_{13}–C_{16}–C_{21}–C_{20}	178.75	173.36	172.68
S_{13}–C_{16}–C_{21}–H_{22}	-2.85	-6.81	-7.29
C_{17}–C_{16}–C_{21}–C_{20}	-0.34	-1.63	-1.05
C_{17}–C_{16}–C_{21}–H_{22}	178.05	178.20	178.97
C_{16}–C_{17}–C_{18}–C_{19}	0.08	0.17	1.14
C_{16}–C_{17}–C_{18}–H_{25}	-179.62	179.03	-178.90
H_{24}–C_{17}–C_{18}–C_{19}	178.69	179.97	-178.91
H_{24}–C_{17}–C_{18}–H_{25}	-1.02	-1.16	1.05
C_{17}–C_{18}–C_{19}–C_{20}	-0.52	-2.21	-2.09
C_{17}–C_{18}–C_{19}–N_{26}	179.93	175.41	178.03
H_{25}–C_{18}–C_{19}–C_{20}	179.20	178.90	177.95
H_{25}–C_{18}–C_{19}–N_{26}	-0.35	-3.49	-1.93
C_{18}–C_{19}–C_{20}–C_{21}	0.53	2.34	1.45
N_{26}–C_{19}–C_{20}–C_{21}	-179.97	-175.04	-178.68
N_{26}–C_{19}–C_{20}–H_{23}	0.38	3.62	1.36
C_{18}–C_{19}–N_{26}–N_{27}	-179.57	179.02	-179.96
C_{20}–C_{19}–N_{26}–N_{27}	0.91	-3.49	0.17
C_{19}–C_{20}–C_{21}–C_{16}	-0.10	-0.45	0.10
C_{19}–C_{20}–C_{21}–H_{22}	-178.48	179.73	-179.92
H_{23}–C_{20}–C_{21}–H_{22}	1.16	1.10	0.04
C_{19}–N_{26}–N_{27}–C_{28}	179.99	175.27	178.96
N_{26}–N_{27}–C_{28}–C_{29}	0.18	-1.50	-0.37
N_{26}–N_{27}–C_{28}–C_{33}	-179.84	-178.75	-179.43
N_{27}–C_{28}–C_{29}–C_{30}	-179.98	-175.56	-178.14
N_{27}–C_{28}–C_{29}–H_{35}	0.03	3.29	1.87
C_{33}–C_{28}–C_{29}–H_{35}	-179.95	-179.53	-179.09
N_{27}–C_{28}–C_{33}–C_{32}	179.98	175.53	178.45
N_{27}–C_{28}–C_{33}–H_{34}	-0.02	-3.01	-1.54
C_{28}–C_{29}–C_{30}–C_{31}	0.00	0.44	0.46
C_{28}–C_{29}–C_{30}–H_{36}	-179.99	179.11	-179.62
H_{35}–C_{29}–C_{30}–C_{31}	179.98	-178.38	-179.55
H_{35}–C_{29}–C_{30}–H_{36}	-0.01	0.29	0.37
C_{29}–C_{30}–C_{31}–C_{32}	-0.02	-2.22	-2.07
C_{29}–C_{30}–C_{31}–O_{41}	179.98	177.81	179.29
H_{36}–C_{30}–C_{31}–C_{32}	179.96	179.06	178.01
H_{36}–C_{30}–C_{31}–O_{41}	-0.04	-0.91	-0.63
C_{30}–C_{31}–C_{32}–C_{33}	0.02	1.93	2.28
C_{30}–C_{31}–C_{32}–C_{37}	-179.95	-179.82	-176.58
O_{41}–C_{31}–C_{32}–C_{33}	-179.98	-178.10	-179.15
O_{41}–C_{31}–C_{32}–C_{37}	0.05	0.14	1.99

Dihedral angle	Calc. (°)		Expt. [114] (°)
	Monomer	Dimer	
C_{30}–C_{31}–O_{41}–H_{42}	180.00	-176.95	-179.65
C_{32}–C_{31}–O_{41}–H_{42}	0.00	3.08	1.74
C_{31}–C_{32}–C_{33}–C_{28}	0.01	0.11	-0.93
C_{31}–C_{32}–C_{33}–H_{34}	-179.99	178.64	179.06
C_{37}–C_{32}–C_{33}–C_{28}	179.98	-178.10	177.92
C_{37}–C_{32}–C_{33}–H_{34}	-0.02	0.43	-2.08
C_{31}–C_{32}–C_{37}–O_{38}	179.94	173.88	172.59
C_{33}–C_{32}–C_{37}–O_{38}	-0.03	-7.92	-6.24
C_{33}–C_{32}–C_{37}–O_{40}	179.98	171.44	173.59
C_{32}–C_{37}–O_{38}–H_{39}	-179.95	-178.55	179.85
O_{40}–C_{37}–O_{38}–H_{39}	0.04	2.10	0.02

Table 5.4 Optimized hydrogen-bond geometry of sulfasalazine.

	D–H···A	D–H (Å)	H···A (Å)	D···A (Å)	D–H···A (°)
Expt. [114]	N–H···O	0.993	1.966	2.948	169.31
	O–H···N	1.005	1.622	2.623	173.24
	O–H···O (intramolecular)	0.910	1.755	2.604	154.11
Calc.	N_{11}–H_{12}···O_{82}	1.026	1.924	2.941	170.53
	N_{53}–H_{54}···O_{40}	1.026	1.924	2.941	170.53
	O_{38}–H_{39}···N_{43}	1.019	1.675	2.692	175.02
	O_{80}–H_{81}···N_1	1.019	1.675	2.692	175.02
	O_{41}–H_{42}···O_{40} (intramolecular monomer)	0.984	1.737	2.611	145.91
	O_{83}–H_{84}···O_{82} (intramolecular)	0.986	1.720	2.597	146.07

5.3 NBO analysis

NBO depicts the importance of hyperconjugative interaction and electron density (ED) transfer from lone pair electrons of the Y atom to the X–H antibonding orbital in the X–H···Y hydrogen bonded system [75]. This $n \rightarrow \sigma^*$ interaction is associated with shift in occupancies i.e., the occupancy of X–H antibonding orbital increases and the lone pair has decreased in occupancy from its monomer value. The increase of electron density in σ*(X–H) weakens the bond, which leads to X–H bond

elongation and red shift in the corresponding X–H stretching frequency. In the present work, NBO analysis is performed for the title compound and the occupancies with their energies for the interacting NBOs have been reported in Table 5.5.

Table 5.5 Occupancies of interacting NBOs of sulfasalazine with their respective energies.

Parameters	Occupancy (e)			Energy (a.u.)		
	Monomer	Dimer	$\Delta_{occ.}$	Monomer	Dimer	ΔE
$n_1(O_{40})$	1.96946	1.95733	-0.01213	-0.72757	-0.73127	-0.00370
$n_2(O_{40})$	1.84242	1.85690	0.01448	-0.31940	-0.31275	0.00665
$\sigma^*(O_{41}–H_{42})$	0.04947	0.05064	0.00117	0.38437	0.39052	0.00615
$\sigma^*(N_{53}–H_{54})$	0.01406	0.03590	0.02184	0.39483	0.41062	0.01579
$n_1(N_{43})$	1.90895	1.85125	-0.05770	-0.35075	-0.38865	-0.03790
$\sigma^*(O_{38}–H_{39})$	0.00962	0.09467	0.08505	0.35739	0.34947	-0.00792
$n_1(N_1)$	1.90895	1.85125	-0.05770	-0.35075	-0.38865	-0.03790
$\sigma^*(O_{80}–H_{81})$	0.00962	0.09467	0.08505	0.35739	0.34947	-0.00792
$n_1(O_{82})$	1.96946	1.95733	-0.01213	-0.72757	-0.73127	-0.00370
$n_2(O_{82})$	1.84242	1.85690	0.01448	-0.31940	-0.31275	0.00665
$\pi(C_{37}–O_{40})$	1.98524	1.99495	0.00971	-0.41765	-1.06645	-0.64880
$\sigma^*(N_{11}–H_{12})$	0.01406	0.03590	0.02184	0.39483	0.41062	0.01579
$\sigma^*(C_{31}–O_{41})$	0.01968	0.01979	0.00011	0.36687	0.37383	0.00696
$\sigma^*(C_{37}–O_{40})$	0.02085	0.02630	0.00545	0.54499	0.52267	-0.02232
$\pi^*(C_{37}–O_{40})$	0.29943	0.34030	0.04087	-0.03135	-0.03143	-0.00008
$\sigma^*(C_{32}–C_{37})$	0.05764	0.05706	-0.00058	0.41098	0.41398	0.00300
$\sigma^*(C_{37}–O_{38})$	0.08188	0.06371	-0.01817	0.33039	0.39285	0.06246
$n_1(N_{11})$	1.81701	1.82059	0.00358	-0.32449	-0.32506	-0.00057
$n_1(N_{26})$	1.95483	1.95390	-0.00093	-0.41789	-0.41540	0.00249
$n_1(N_{27})$	1.95348	1.95330	-0.00018	-0.41721	-0.41436	0.00285
$n_1(O_{38})$	1.97730	1.96760	-0.00970	-0.64818	-0.58528	0.06290
$n_2(O_{38})$	1.81655	1.76466	-0.05189	-0.36452	-0.33856	0.02596

The second order perturbative estimates of donor-acceptor interactions of sulfasalazine monomer and dimer have been summarized in Table 5.6. An intramolecular $O_{41}–H_{42}\cdots O_{40}$ interaction formed between the hydroxyl group and carbonyl oxygen of carboxylic acid group is confirmed by the energetic contribution [$n_2(O_{40})\rightarrow\sigma^*(O_{41}–H_{42})$] of 15.26 kcalmol^{-1}. The stabilization energy E(2) of 5.03 and 4.11 kcal mol^{-1} quantifies the level of hyperconjugative interactions $n_1(O_{40})\rightarrow\sigma^*(N_{53}–H_{54})$, $n_1(O_{82})\rightarrow\sigma^*(N_{11}–H_{12})$ and $n_2(O_{40})\rightarrow\sigma^*(N_{53}–H_{54})$, $n_2(O_{82})\rightarrow\sigma^*(N_{11}–H_{12})$ respectively. The charge transfer from the lone pair electrons (O_{40} and O_{82}) to the $N_{53}–H_{54}$ and $N_{11}–H_{12}$ antibonding orbitals increases the occupancy (~0.0218e) upon dimerization. Consequently, the bonds $N_{53}–H_{54}$ and $N_{11}–H_{12}$ weaken and this supports the bond elongation discussed in geometry. The magnitude of charge transferred from lone pair electrons of $n_1(N_{43})$ and $n_1(N_1)$ to the $O_{38}–H_{39}$ and $O_{80}–H_{81}$ antibonding orbitals is significantly increased (~0.0851e) from monomer to dimer.

Table 5.6 Second order perturbation theory analysis of Fock matrix in NBO basis.

Donor (i)	Acceptor (j)	E(2)[a] (Kcalmol^{-1})	E(j)-E(i)[b] (a.u.)	F(i, j)[c] (a.u.)
Within unit 1				
$\pi(N_1–C_2)$	$\pi^*(C_3–C_4)$	11.53	0.33	0.056
$\pi(N_1–C_2)$	$\pi^*(C_5–C_6)$	26.45	0.33	0.084
$\pi(C_{18}–C_{19})$	$\pi^*(N_{26}–N_{27})$	18.96	0.23	0.062
$\pi(C_{20}–C_{21})$	$\pi^*(C_{18}–C_{19})$	20.61	0.29	0.069
$n_1(N_{11})$	$\pi^*(N_1–C_2)$	23.05	0.31	0.082
$n_2(O_{38})$	$\pi^*(C_{37}–O_{40})$	47.47	0.33	0.116
$n_2(O_{40})$	$\sigma^*(O_{41}–H_{42})$	15.26	0.70	0.095
$\pi^*(N_1–C_2)$	$\pi^*(C_5–C_6)$	118.38	0.02	0.079
$\pi^*(C_{16}–C_{17})$	$\pi^*(C_{18}–C_{19})$	249.01	0.01	0.086

$\pi^*(C_{16}–C_{17})$	$\pi^*(C_{20}–C_{21})$	144.46	0.02	0.079
From unit 1 to unit 2				
$n_1(N_1)$	$\sigma^*(O_{80}–H_{81})$	36.97	0.74	0.149
$n_1(O_{40})$	$\sigma^*(N_{53}–H_{54})$	5.03	1.14	0.068
$n_2(O_{40})$	$\sigma^*(N_{53}–H_{54})$	4.11	0.72	0.050
$\pi(C_{37}–O_{40})$	$\sigma^*(N_{53}–H_{54})$	0.87	0.82	0.024
$n_1(N_{43})$	$\sigma^*(C_{37}–O_{38})$	0.10	0.78	0.008
From unit 2 to unit 1				
$n_1(N_{43})$	$\sigma^*(O_{38}–H_{39})$	36.97	0.74	0.149
$\sigma(N_{53}–H_{54})$	$\sigma^*(C_{37}–O_{40})$	0.10	1.20	0.010
$n_1(N_{43})$	$\sigma^*(C_{37}–O_{38})$	0.10	0.78	0.008
$n_1(O_{82})$	$\sigma^*(N_{11}–H_{12})$	5.03	1.14	0.068
$n_2(O_{82})$	$\sigma^*(N_{11}–H_{12})$	4.11	0.72	0.050
$n_2(O_{82})$	$\sigma^*(N_{11}–S_{13})$	0.06	0.41	0.005
Within unit 2				
$\pi(N_{43}–C_{44})$	$\pi^*(C_{45}–C_{46})$	10.35	0.35	0.054
$\pi(N_{43}–C_{44})$	$\pi^*(C_{47}–C_{48})$	25.09	0.34	0.083
$\pi(C_{45}–C_{46})$	$\pi^*(N_{43}–C_{44})$	31.75	0.25	0.082
$\pi(C_{58}–C_{59})$	$\pi^*(C_{62}–C_{63})$	19.36	0.31	0.069
$\pi(C_{60}–C_{61})$	$\pi^*(C_{58}–C_{59})$	24.33	0.27	0.072
$n_2(O_{82})$	$\sigma^*(O_{83}–H_{84})$	14.98	0.70	0.094

[a]E(2) is the energy of hyperconjugative interactions.
[b]Energy difference between donor and acceptor i and j NBO orbitals.
[c]F(i,j) is the Fock matrix element between i and j NBO orbitals.

Alike the N–H···O interaction mentioned earlier, O–H···N interaction weakens the bonds, which leads to bond elongation ($O_{38}–H_{39}$ and $O_{80}–H_{81}$) and the corresponding stretching frequency is redshifted. The stabilization energy E(2) corresponding to this intermolecular interactions $n_1(N_{43}) \rightarrow \sigma^*(O_{38}–H_{39})$ and $n_1(N_1) \rightarrow \sigma^*(O_{80}–H_{81})$ is obtained as 36.97 kcalmol^{-1}. From the stabilization energies obtained it is clear that the strength of hydrogen bond is in the order $O–H\cdots N > O–H\cdots O > N–H\cdots O$. The charge transfer from $\sigma(N_{53}–H_{54}) \rightarrow$

σ*(C_{37}–O_{40}) is associated with the bond lengthening of C_{37}–O_{40} bond. The hyperconjugative interaction $n_1(N_{43}) \rightarrow$ σ*(C_{37}–O_{38}) of low energy contribution (0.10 kcalmol^{-1}) reduces the bond length C_{37}–O_{38} upon dimerization.

5.4 Vibrational analysis

Vibrational assignments of sulfasalazine have been made based on normal coordinate analysis followed by SQM procedure. The title compound consists of 42 atoms and hence 120 modes of vibration. Scale factors have been refined with an RMS error of 6.53 cm^{-1} between the experimental and SQM force field frequencies of the title compound. Internal valence coordinates [71] of sulfasalazine monomer has been defined in Table 5.7. Force constants of the symmetry coordinates and the scale factors used are given in Table 5.8. The FT-IR and FT-Raman spectra of the title compound are shown in Fig. 5.4 and Fig. 5.5 (3600-2500 cm^{-1} region), Fig. 5.6 (2500-50 cm^{-1} region) respectively. The vibrational analyses of various functional groups are shown in Table 5.9.

Table 5.7 Definition of internal valence coordinates of sulfasalazine.

No.	Symbol	Type	Definition
Stretching			
1–16	R_i	C-C (ring)	C_2-C_3, C_3-C_4, C_4-C_5, C_5-C_6, C_{16}-C_{17}, C_{17}-C_{18}, C_{18}-C_{19}, C_{19}-C_{20}, C_{20}-C_{21}, C_{21}-C_{16}, C_{28}-C_{29}, C_{29}-C_{30}, C_{30}-C_{31}, C_{31}-C_{32}, C_{32}-C_{33}, C_{33}-C_{28}
17–18	R_i	C-N (ring A)	C_6-N_1, N_1-C_2
19–29	r_i	C-H (ring)	C_6-H_7, C_5-H_8, C_4-H_9, C_3-H_{10}, C_{21}-H_{22}, C_{20}-H_{23}, C_{17}-H_{24}, C_{18}-H_{25}, C_{29}-H_{35}, C_{30}-H_{36}, C_{33}-H_{34}
30	P_i	N-H (sulfonamide)	N_{11}-H_{12}
31	ξ_i	C-N (sulfonamide)	C_2-N_{11}
32	ξ_i	N-S (sulfonamide)	N_{11}-S_{13}

No.	Symbol	Type	Definition
33–34	R_i	S-O (sulfonamide)	S_{13}-O_{14}, S_{13}-O_{15}
35	r_i	S-C (sulfonamide)	S_{13}-C_{16}
36	r_i	C-N (chain)	C_{19}-N_{26}
37	P_i	N-N (chain)	N_{26}-N_{27}
38	r_i	N-C (chain)	N_{27}-C_{28}
39	r_i	C-C (carboxylic)	C_{32}-C_{37}
40	Q_i	C=O (carboxylic)	C_{37}-O_{40}
41	Q_i	C-O (carboxylic)	C_{37}-O_{38}
42	P_i	O-H (carboxylic)	O_{38}-H_{39}
43	Q_i	C-O (hydroxy)	C_{31}-O_{41}
44	P_i	O-H (hydroxy)	O_{41}-H_{42}
Bending			
45–47	α_i	C-N-C (ring A)	C_6-N_1-C_2, N_1-C_2-C_3, C_5-C_6-N_1
48–62	α_i	C-C-C (ring)	C_2-C_3-C_4, C_3-C_4-C_5, C_4-C_5-C_6, C_{21}-C_{16}-C_{17}, C_{16}-C_{17}-C_{18}, C_{17}-C_{18}-C_{19}, C_{18}-C_{19}-C_{20}, C_{19}-C_{20}-C_{21}, C_{20}-C_{21}-C_{16}, C_{33}-C_{28}-C_{29}, C_{28}-C_{29}-C_{30}, C_{29}-C_{30}-C_{31}, C_{30}-C_{31}-C_{32}, C_{31}-C_{32}-C_{33}, C_{32}-C_{33}-C_{28}
63–84	β_i	H-C-C (ring)	H_7-C_6-N_1, H_7-C_6-C_5, H_8-C_5-C_4, H_8-C_5-C_6, H_9-C_4-C_3, H_9-C_4-C_5, H_{10}-C_3-C_2, H_{10}-C_3-C_4, H_{22}-C_{21}-C_{16}, H_{22}-C_{21}-C_{20}, H_{23}-C_{20}-C_{21}, H_{23}-C_{20}-C_{19}, H_{24}-C_{17}-C_{18}, H_{24}-C_{17}-C_{16}, H_{25}-C_{18}-C_{19}, H_{25}-C_{18}-C_{17}, H_{34}-C_{33}-C_{28}, H_{34}-C_{33}-C_{32}, H_{35}-C_{29}-C_{30}, H_{35}-C_{29}-C_{28}, H_{36}-C_{30}-C_{31}, H_{36}-C_{30}-C_{29}
85	θ_i	N-C-N	N_{11}-C_2-N_1
86	θ_i	N-C-C	N_{11}-C_2-C_3
87	θ_i	C-N-H (sulfonamide)	C_2-N_{11}-H_{12}
88	θ_i	H-N-S (sulfonamide)	H_{12}-N_{11}-S_{13}
89	α_i	C-N-S (sulfonamide)	C_2-N_{11}-S_{13}
90	α_i	O-S-O (sulfonamide)	O_{14}-S_{13}-O_{15}
91	γ_i	N-S-C	N_{11}-S_{13}-C_{16}
92–93	β_i	O-S-C	O_{14}-S_{13}-C_{16}, O_{15}-S_{13}-C_{16}
94–95	β_i	O-S-N	O_{14}-S_{13}-N_{11}, O_{15}-S_{13}-N_{11}
96–97	β_i	S-C-C (chain)	S_{13}-C_{16}-C_{17}, S_{13}-C_{16}-C_{21}
98–99	α_i	N-C-C (chain)	N_{26}-C_{19}-C_{20}, N_{26}-C_{19}-C_{18}

No.	Symbol	Type	Definition
100	α_i	C-N-N (chain)	C_{19}-N_{26}-N_{27}
101	α_i	N-N-C (chain)	N_{26}-N_{27}- C_{28}
102–103	β_i	N-C-C (ring C)	N_{27}-C_{28}-C_{29}, N_{27}-C_{28}-C_{33}
104–105	α_i	C-C-C (carboxylic)	C_{37}-C_{32}-C_{33}, C_{37}-C_{32}-C_{31}
106–107	ϕ_i	C-C-O (carboxylic)	C_{32}-C_{37}-O_{40}, C_{32}-C_{37}-O_{38}
108	ϕ_i	O-C-O (carboxylic)	O_{40}-C_{37}-O_{38}
109	β_i	C-O-H (carboxylic)	C_{37}-O_{38}-H_{39}
110	α_i	C-O-H (hydroxyl)	C_{31}-O_{41}-H_{42}
111–112	β_i	O-C-C (hydroxyl)	O_{41}-C_{31}-C_{32}, O_{41}-C_{31}-C_{30}
Out-of-plane bending (wagging)			
113–123	ω_i	C-H (ring)	H_7-C_6-C_5-N_1, H_8-C_5-C_4-C_6, H_9-C_4-C_3-C_5, H_{10}-C_3-C_2-C_4, H_{22}-C_{21}-C_{16}-C_{20}, H_{23}-C_{20}-C_{21}-C_{19}, H_{24}-C_{17}-C_{18}-C_{16}, H_{25}-C_{18}-C_{19}-C_{17}, H_{34}-C_{33}-C_{28}-C_{32}, H_{35}-C_{29}-C_{30}-C_{28}, H_{36}-C_{30}-C_{31}-C_{29}
124	ω_i	C-N (sulfonamide)	N_{11}-C_2-N_1-C_3
125	ω_i	N-H (sulfonamide)	C_2-N_{11}-H_{12}-S_{13}
126	ω_i	S-C (sulfonamide)	S_{13}-C_{16}-C_{17}-C_{21}
127	ω_i	C-N (chain)	N_{26}-C_{19}-C_{20}-C_{18}
128	ω_i	N-C (chain)	N_{27}-C_{28}-C_{29}-C_{33}
129	ω_i	C-C (carboxylic)	C_{37}-C_{32}-C_{33}-C_{31}
130	ω_i	C-O (carboxylic)	C_{32}-C_{37}-O_{40}-O_{38}
131	ω_i	C-O (hydroxyl)	O_{41}-C_{31}-C_{32}-C_{30}
Torsion			
132–149	τ_i	C-C (ring)	C_6-N_1-C_2-C_3, N_1-C_2-C_3-C_4, C_2-C_3-C_4-C_5, C_3-C_4-C_5-C_6, C_4-C_5-C_6-N_1, C_5-C_6-N_1-C_2, C_{21}-C_{16}-C_{17}-C_{18}, C_{16}-C_{17}-C_{18}-C_{19}, C_{17}-C_{18}-C_{19}-C_{20}, C_{18}-C_{19}-C_{20}-C_{21}, C_{19}-C_{20}-C_{21}-C_{16}, C_{20}-C_{21}-C_{16}-C_{17}, C_{33}-C_{28}-C_{29}-C_{30}, C_{28}-C_{29}-C_{30}-C_{31}, C_{29}-C_{30}-C_{31}-C_{32}, C_{30}-C_{31}-C_{32}-C_{33}, C_{31}-C_{32}-C_{33}-C_{28}, C_{32}-C_{33}-C_{28}-C_{29}
150–153	τ_i	C-N (ring)	N_1-C_2-N_{11}-H_{12}, N_1-C_2-N_{11}-S_{13}, C_3-C_2-N_{11}-H_{12}, C_3-C_2-N_{11}-S_{13}
154–159	τ_i	N-S (sulfonamide)	C_2-N_{11}-S_{13}-O_{14}, C_2-N_{11}-S_{13}-O_{15}, C_2-N_{11}-S_{13}-C_{16}, H_{12}-N_{11}-S_{13}-O_{14}, H_{12}-N_{11}-S_{13}-

No.	Symbol	Type	Definition
			O_{15}, H_{12}-N_{11}-S_{13}-C_{16}
160–165	τ_i	S-C (sulfonamide)	N_{11}-S_{13}-C_{16}-C_{17}, N_{11}-S_{13}-C_{16}-C_{21}, O_{14}-S_{13}-C_{16}-C_{17}, O_{14}-S_{13}-C_{16}-C_{21}, O_{15}-S_{13}-C_{16}-C_{17}, O_{15}-S_{13}-C_{16}-C_{21}
166	τ_i	N-N (chain)	C_{19}-N_{26}-N_{27}-C_{28}
167–168	τ_i	C-N (chain)	C_{18}-C_{19}-N_{26}-N_{27}, C_{20}-C_{19}-N_{26}-N_{27}
169–170	τ_i	N-C (chain)	N_{26}-N_{27}-C_{28}-C_{29}, N_{26}-N_{27}-C_{28}-C_{33}
171–174	τ_i	C-C (chain)	C_{31}-C_{32}-C_{37}-O_{38}, C_{31}-C_{32}-C_{37}-O_{40}, C_{33}-C_{32}-C_{37}-O_{38}, C_{33}-C_{32}-C_{37}-O_{40}
175–176	τ_i	C-O (carboxylic)	C_{32}-C_{37}-O_{38}-H_{39}, O_{40}-C_{37}-O_{38}-H_{39}
177–178	τ_i	C-O (hydroxyl)	C_{30}-C_{31}-O_{41}-H_{42}, C_{32}-C_{31}-O_{41}-H_{42}

5.4.1 Pyridine ring vibrations

The C-H stretching vibration of nitrogen heterocyclic aromatic compounds gives rise to bands in the region 3100 – 3010 cm^{-1} [103]. The medium intense bands at 3117 cm^{-1} and 3036 cm^{-1} in the Raman spectrum is assigned to C-H stretching vibrational modes of pyridine ring (Py) in the title compound. The C-H stretching modes of Py are observed at 3079 cm^{-1} and 3044 cm^{-1} in the IR spectrum. The C-C stretching vibration of monosubstituted pyridine ring is observed in the region 1615 – 1575 cm^{-1} [103]. A strong band at 1586 cm^{-1} in the Raman spectrum is assigned to C-C stretching mode of Py. The CH out-of-plane bending usually appears in the region 780 – 740 cm^{-1} [122, 123]. The band at 767 cm^{-1} in the IR is assigned to C-H wagging mode cm^{-1}. The strong band at 1413 cm^{-1} in the IR spectrum is assigned to C-N stretching mode of pyridine ring in the sulfasalazine compound.

Table 5.8 Definition of local symmetry coordinates (much like the natural internal coordinates) and the corresponding force constant (mdyne/A°) of sulfasalazine with scale factors used.

No.	Symbol	Definition	Scale factors	Force constants (mdyne/Å)
Stretching				
1-4	Py[νCC]	R_1, R_2, R_3, R_4	0.937	6.251
5-10	PhA[νCC]	R_5, R_6, R_7, R_8, R_9, R_{10}	0.937	6.059
11-16	PhB[νCC]	R_{11}, R_{12}, R_{13}, R_{14}, R_{15}, R_{16}	0.937	5.852
17-18	Py[νCN]	R_{17}, R_{18}	0.968	7.368
19-22	Py[νCH]	r_{19}, r_{20}, r_{21}, r_{22}	0.926	5.070
23-26	PhA[νCH]	r_{23}, r_{24}, r_{25}, r_{26}	0.926	5.193
27-29	PhB[νCH]	r_{27}, r_{28}, r_{29}	0.926	5.192
30	νNH	P_{30}	0.918	6.442
31	NH_{ss}	$(\xi_{31}+\xi_{32})/\sqrt{2}$	0.881	4.568
32	NH_{ips}	$(\xi_{31}-\xi_{32})/\sqrt{2}$	0.881	3.681
33	SO_{2ss}	$(R_{33}+R_{34})/\sqrt{2}$	1.007	9.416
34	SO_{2ips}	$(R_{33}-R_{34})/\sqrt{2}$	1.007	9.580
35	νSC	r_{35}	0.854	2.577
36	PhA[νCN]	r_{36}	0.968	5.059
37	νNN	P_{37}	0.942	9.627
38	PhB[νCN]	r_{38}	1.019	5.553
39	COOH[νCC]	r_{39}	0.936	4.990
40	ν(C=O)	Q_{40}	0.927	10.901
41	COOH[νCO]	Q_{41}	1.108	7.108
42	COOH[νOH]	P_{42}	0.904	7.182
43	COH[νCO]	Q_{43}	0.962	6.974
44	COH[νOH]	P_{44}	0.904	5.866
Bending				
45	Py_{trid}	$(\alpha_{45}-\alpha_{46}+\alpha_{48}-\alpha_{49}+\alpha_{50}-\alpha_{47})/\sqrt{6}$	0.924	1.247
46	Py_{asyd}	$(2\alpha_{45}-\alpha_{46}-\alpha_{48}+2\alpha_{49}-\alpha_{50}-\alpha_{47})/\sqrt{12}$	1.000	1.290
47	Py_{asydo}	$(\alpha_{45}-\alpha_{46}+\alpha_{49}-\alpha_{50})/2$	0.918	1.372
48	PhA_{trid}	$(\alpha_{51}-\alpha_{52}+\alpha_{53}-\alpha_{54}+\alpha_{55}-\alpha_{56})/\sqrt{6}$	0.924	1.199
49	PhA_{asyd}	$(2\alpha_{51}-\alpha_{52}-\alpha_{53}+2\alpha_{54}-\alpha_{55}-$	1.000	1.395

No.	Symbol	Definition	Scale factors	Force constants (mdyne/Å)
		$\alpha_{56})/\sqrt{12}$		
50	PhA_{asydo}	$(\alpha_{51}-\alpha_{52}+\alpha_{54}-\alpha_{55})/2$	0.918	1.148
51	PhB_{trid}	$(\alpha_{57}-\alpha_{58}+\alpha_{59}-\alpha_{60}+\alpha_{61}-\alpha_{62})/\sqrt{6}$	0.924	1.255
52	PhB_{asyd}	$(2\alpha_{57}-\alpha_{58}-\alpha_{59}+2\alpha_{60}-\alpha_{61}-\alpha_{62})/\sqrt{12}$	1.000	1.462
53	PhB_{asydo}	$(\alpha_{57}-\alpha_{58}+\alpha_{60}-\alpha_{61})/2$	0.918	1.235
54-57	Py[δCH]	$(\beta_{64}-\beta_{63})/\sqrt{2}$, $(\beta_{65}-\beta_{66})/\sqrt{2}$, $(\beta_{67}-\beta_{68})/\sqrt{2}$, $(\beta_{69}-\beta_{70})/\sqrt{2}$	0.887	0.454
58-61	PhA[δCH]	$(\beta_{71}-\beta_{72})/\sqrt{2}$, $(\beta_{73}-\beta_{74})/\sqrt{2}$, $(\beta_{75}-\beta_{76})/\sqrt{2}$, $(\beta_{77}-\beta_{78})/\sqrt{2}$	0.887	0.450
62-64	PhB[δCH]	$(\beta_{79}-\beta_{80})/\sqrt{2}$, $(\beta_{81}-\beta_{82})/\sqrt{2}$, $(\beta_{83}-\beta_{84})/\sqrt{2}$	0.887	0.450
65	Py[δCN]	$(\theta_{85}-\theta_{86})/\sqrt{2}$	1.278	1.626
66	NH_{roc}	$(\theta_{87}-\theta_{88})/\sqrt{2}$	0.911	0.524
67	δCNS	$(2\alpha_{89}-\beta_{87}-\beta_{88})/\sqrt{6}$	0.911	0.965
68	SO_{2sci}	$(5\alpha_{90}+\gamma_{91})/\sqrt{26}$	0.889	1.603
69	SNC_{sci}	$(\alpha_{90}+5\gamma_{91})/\sqrt{26}$	0.889	1.259
70	SO_{2roc}	$(\beta_{92}-\beta_{93}+\beta_{94}-\beta_{95})/2$	0.889	1.301
71	SO_{2wag}	$(\beta_{92}+\beta_{93}-\beta_{94}-\beta_{95})/2$	0.889	1.684
72	SO_{2twi}	$(\beta_{92}-\beta_{93}-\beta_{94}+\beta_{95})/2$	0.889	0.969
73	δSC	$(\beta_{96}-\beta_{97})/\sqrt{2}$	0.889	0.787
74	PhA[δCN]	$(\beta_{98}-\beta_{99})/\sqrt{2}$	1.278	1.434
75	δNN1	α_{100}	0.788	1.494
76	δNN2	α_{101}	0.788	1.467
77	PhB[δCN]	$(\beta_{102}-\beta_{103})/\sqrt{2}$	1.278	1.383
78	COOH[δCC]	$(\alpha_{104}-\alpha_{105})/\sqrt{2}$	0.896	1.590
79	CO_{ipb}	$(\phi_{106}-\phi_{108})/\sqrt{2}$	0.896	1.419
80	COOH[δCCO]	$(2\phi_{107}-\phi_{106}-\phi_{108})/\sqrt{6}$	0.896	1.143
81	COOH[δOH]	β_{109}	0.896	0.683
82	COH[δOH]	α_{110}	0.896	1.000
83	COH[δCO]	$(\beta_{111}-\beta_{112})/\sqrt{2}$	0.896	1.275
84-87	Py[gCH]	ω_{113}, ω_{114}, ω_{115}, ω_{116}	0.968	0.437
88-91	PhA[gCH]	ω_{117}, ω_{118}, ω_{119}, ω_{120}	0.968	0.457
92-94	PhB[gCH]	ω_{121}, ω_{122}, ω_{123}	0.968	0.433
95	Py[gCN]	ω_{124}	0.968	0.647

No.	Symbol	Definition	Scale factors	Force constants (mdyne/Å)
96	gNH	ω_{125}	0.911	0.138
97	gSC	ω_{126}	0.889	0.386
98	PhA[gCN]	ω_{127}	0.968	0.609
99	PhB[gCN]	ω_{128}	0.968	0.549
100	COOH[gCC]	ω_{129}	1.030	0.614
101	COOH[gCO]	ω_{130}	1.030	0.596
102	COH[gCO]	ω_{131}	1.030	0.921
Torsion				
103	Py_{puck}	$(\tau_{132}-\tau_{133}+\tau_{134}-\tau_{135}+\tau_{136}-\tau_{137})/\sqrt{6}$	0.955	0.345
104	Py_{asyt}	$(\tau_{132}-\tau_{134}+\tau_{135}-\tau_{137})/2$	0.877	0.257
105	Py_{asyto}	$(-\tau_{132}+2\tau_{133}-\tau_{134}-\tau_{135}+2\tau_{136}-\tau_{137})/\sqrt{12}$	1.050	0.279
106	PhA_{puck}	$(\tau_{138}-\tau_{139}+\tau_{140}-\tau_{141}+\tau_{142}-\tau_{143})/\sqrt{6}$	0.955	0.371
107	PhA_{asyt}	$(\tau_{138}-\tau_{140}+\tau_{141}-\tau_{143})/2$	0.877	0.275
108	PhA_{asyto}	$(-\tau_{138}+2\tau_{139}-\tau_{140}-\tau_{141}+2\tau_{142}-\tau_{143})/\sqrt{12}$	1.050	0.361
109	PhB_{puck}	$(\tau_{144}-\tau_{145}+\tau_{146}-\tau_{147}+\tau_{148}-\tau_{149})/\sqrt{6}$	0.955	0.385
110	PhB_{asyt}	$(\tau_{144}-\tau_{146}+\tau_{147}-\tau_{149})/2$	0.877	0.318
111	PhB_{asyto}	$(-\tau_{144}+2\tau_{145}-\tau_{146}-\tau_{147}+2\tau_{148}-\tau_{149})/\sqrt{12}$	1.050	0.389
112	τNH	$(\tau_{150}+\tau_{151}+\tau_{152}+\tau_{153})/2$	0.925	0.042
113	τNS	$(\tau_{154}+\tau_{155}+\tau_{156}+\tau_{157}+\tau_{158}+\tau_{159})/\sqrt{6}$	0.925	0.025
114	τSC	$(\tau_{160}+\tau_{161}+\tau_{162}+\tau_{163}+\tau_{164}+\tau_{165})/\sqrt{6}$	0.925	0.011
115	τNN	τ_{166}	0.925	0.340
116	τCN	$(\tau_{167}+\tau_{168})/\sqrt{2}$	0.925	0.020
117	τNC	$(\tau_{169}+\tau_{170})/\sqrt{2}$	0.925	0.040
118	τCC	$(\tau_{171}+\tau_{172}+\tau_{173}+\tau_{174})/2$	0.925	0.065
119	τCOOH	$(\tau_{175}+\tau_{176})/\sqrt{2}$	0.925	0.075
120	τCOH	$(\tau_{177}+\tau_{178})/\sqrt{2}$	0.925	0.150

5.4.2 Phenyl ring vibrations

The normal modes of p-disubstituted (Ph A) and asymmetric trisubstituted (Ph B) phenyl rings were made according to Wilson's numbering scheme [99]. The modes 2, 20a and 20b are classified as the C-H stretching modes of the substituted phenyl rings. The strong band at 3069 cm^{-1} in the Raman is assigned to mode 2 of Ph A and Ph B. The mode 20a of Ph A is observed as a medium intense band in the Raman spectrum at 3090 cm^{-1}. The normal modes 8a, 8b, 19a, 19b and 14 are assigned to C-C stretching vibrations of p-disubstituted and asymmetric trisubstituted phenyl rings. The mode 8b of p-disubstituted phenyl ring appears in the region 1552 – 1605 cm^{-1}. The mode 8b of p-disubstituted Ph A is observed as a weak band at 1542 cm^{-1} in the Raman spectrum. The mode 8b is found at a higher wavenumber than 8a. The modes 8a and 8b of asymmetric trisubstituted phenyl ring appears in the region 1560 – 1610 cm^{-1} and 1571 – 1642 cm^{-1} respectively. The strong intense band observed at 1591 cm^{-1} in the IR is assigned to 8b mode and the weak band at 1542 cm^{-1} in the Raman spectrum is assigned to 8a mode of Ph B. The medium band observed at 1487 cm^{-1} in the IR is assigned to the 19b mode of Ph B and the counterpart in the Raman spectrum occurs at 1490 cm^{-1}. The mode 14 of Ph A is observed at 1281 and 1272 cm^{-1} in the IR and Raman spectra respectively. In p-disubstituted phenyl ring the C-H in- plane bending modes are 3, 9a, 18a and 18b. The in-plane vibration mode 3 usually appears in the region 1260 – 1313 cm^{-1}. The strong intense band at 1119 cm^{-1} in the Raman and medium intense band at 1115 cm^{-1} in the IR is assigned to mode 18b of Ph A. Medium intense band at 1232 cm^{-1} in the IR is assigned to mode 3 of Ph B. The weak band observed at 1050 cm^{-1} in the IR is assigned to the 18b mode of Ph B and the counterpart in the Raman spectrum occurs at 1048 cm^{-1}.

5.4.3 Sulfonamide group vibrations

The sulfasalazine molecule contains the secondary sulfonamide (SO_2NH) group. A strong intermolecular hydrogen bonding (N–H···O) is formed between the N–H of sulfonamide group of one molecule with the C=O of carboxylic acid group of another molecule. The calculated N–H stretching vibration is obtained at 3406 cm^{-1} (Table 5.9) as a medium intense band in the IR spectrum. In the title compound N–H stretching vibration is observed as a strong peak at 3406 cm^{-1} with high intensity. The asymmetric and symmetric SO_2 stretching vibrations usually occur in the region 1360 – 1315 cm^{-1} and 1180 – 1140 cm^{-1} respectively [103]. It is observed that the SO_2 in-plane stretching vibration is observed as a strong band in IR at 1357 cm^{-1} and a weak band at 1360 cm^{-1} in the Raman spectrum. The symmetric stretching is observed at 1132 cm^{-1} in the IR spectrum. The medium intense band at 509 cm^{-1} in IR is assigned to SO_2 scissoring vibration which usually appears in the region 586 – 504 cm^{-1}. SO_2 wagging vibration occurs in the region 551 – 438 cm^{-1} [30]. In the IR spectrum SO_2 wagging mode is observed at 591 cm^{-1}.

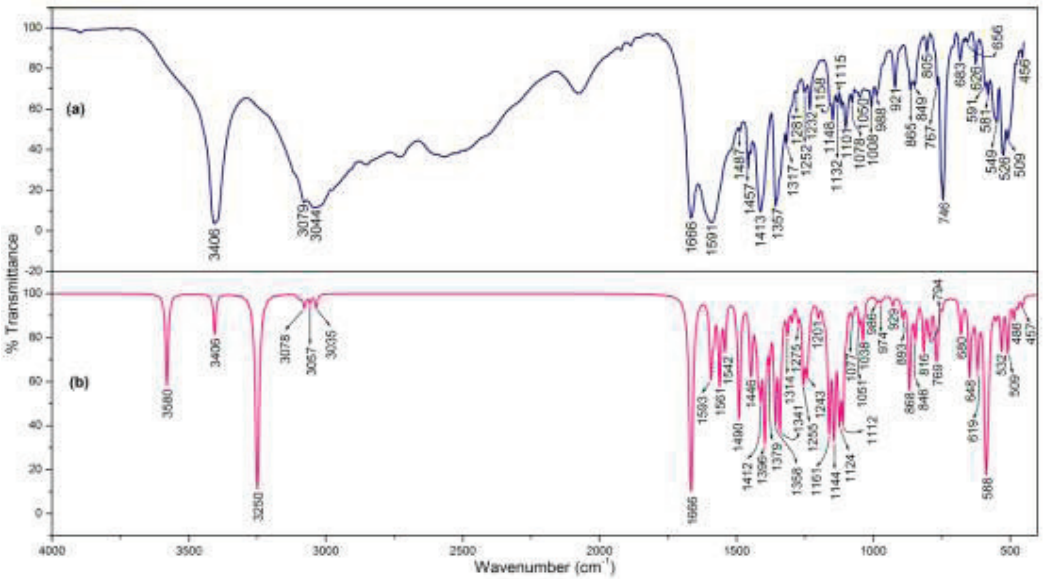

Fig. 5.4 (a) Experimental and (b) simulated IR spectra of sulfasalazine.

5.4.4 Hydroxyl group vibrations

The hydroxyl group vibrations are the stretching and bending vibrations of the CO and OH moieties. The OH stretching vibration of a non-hydrogen bonded molecule appears as a sharp band above 3600 cm^{-1} while that of hydrogen bonded (intramolecular hydrogen bonding) molecule is broadened and shifted to 3200 – 2500 cm^{-1} [30]. In the sulfasalazine compound the intramolecular hydrogen bonding is formed by the interaction between OH proton and the lone-pair oxygen atom of carboxylic group. Intramolecular hydrogen bonding is formed by chelation making a six membered ring structure. The sharp band at 3250 cm^{-1} in the theoretical IR spectra corresponds to OH stretching vibration. This vibration is observed as a redshifted broad band around 3000 cm^{-1} indicating the strength of $O_{41}–H_{42}\cdots O_{40}$ intramolecular hydrogen bond. The medium band at 1297 cm^{-1} in the FT-Raman spectra corresponds to CO stretching vibration. The C–C–O out-of-plane bending vibration is observed as a medium intense band at 549 cm^{-1} in the FT-IR spectrum.

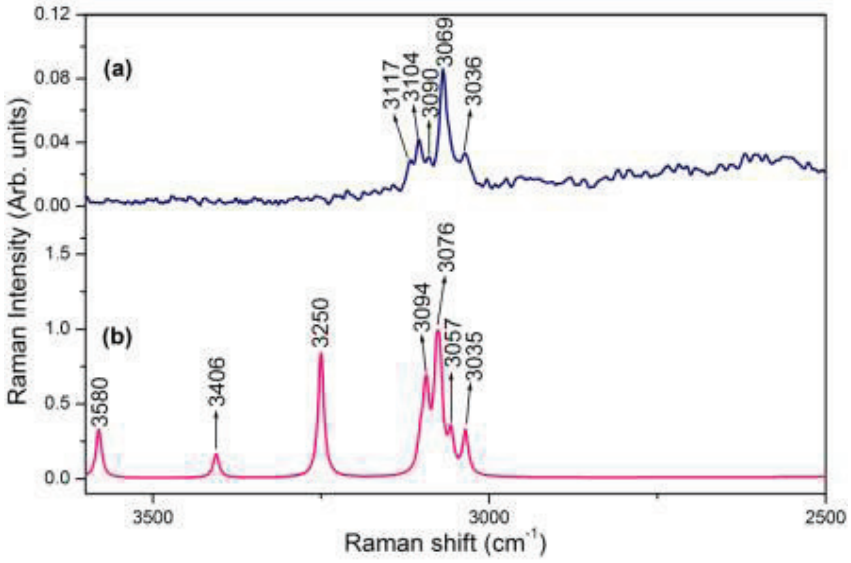

Fig. 5.5 (a) Experimental and (b) simulated Raman spectra of sulfasalazine (3600-2500 cm^{-1} region).

5.4.5 Carboxylic acid group vibrations

The carboxylic acid group vibrations are the vibrations of a carbonyl group (C=O) and a hydroxyl group (OH). The O–H stretching band of the carboxylic acid is observed as a broad, intense peak in the region 3500 to 2500 cm^{-1} [101] in FT-IR spectra. The broad and redshifted shallow appearance in the region 3200 – 2500 cm^{-1} is due to the strong O–H···N (O_{38}–H_{39}···N_{43} and O_{80}–H_{81}···N_1) intermolecular interaction in the crystalline state. Strong and intense band at 3580 cm^{-1} in the theoretical spectra is assigned to O–H stretching of sulfasalazine monomer. The aromatic C=O stretch of carboxylic acids is expected in the region 1710 – 1680 cm^{-1}. The hydrogen bonded carboxylic acid has a center of symmetry so that the vibration will be Raman-active only when the two monomers vibrate in-phase (symmetric) and the vibration will be IR-active only when the molecules vibrate out-of-phase (antisymmetric). The antisymmetric and symmetric C=O stretching is expected in the region 1740 – 1660 cm^{-1} in IR and 1687 – 1625 cm^{-1} in Raman spectra [30] respectively. Since sulfasalazine molecules form a centrosymmetric dimer the C=O antisymmetric stretching is observed as very strong band in IR at 1666 cm^{-1} and it is inactive in the Raman. The symmetric C=O stretching is observed at 1679 cm^{-1} in Raman as a very weak band which is absent in the FT-IR spectrum.

Table 5.9 Vibrational assignment of sulfasalazine by normal coordinate analysis based on SQM force field calculations.

Experimental (cm^{-1})		Calculated {B3LYP/6-311G(d, p)}			
υ_{IR}	υ_{Raman}	υ_{Scaled} (cm^{-1})	IR intensity (%)	Raman intensity (%)	Assignment (% PED, internal coordinates having contribution ≥10% are shown)
-	-	3580	23.63	0.06	COOH[νOH(100)]
3406	-	3406	8.89	0.03	νNH(100)
-	-	3250	95.15	0.16	COH[νOH(100)]

Experimental (cm^{-1})		Calculated {B3LYP/6-311G(d, p)}			
υ_{IR}	υ_{Raman}	υ_{Scaled} (cm^{-1})	IR intensity (%)	Raman intensity (%)	Assignment (% PED, internal coordinates having contribution ≥10% are shown)
-	3117	3102	0.33	0.03	Py[νCH(99)]
-	3104	3097	0.14	0.03	PhA[νCH(99)]
-	-	3095	0.13	0.01	PhB[νCH(99)]
-	3090	3093	0.07	0.04	PhA[νCH(99)]
-	-	3093	0.63	0.04	PhB[νCH(99)]
3079	-	3079	2.36	0.10	Py[νCH(99)]
-	-	3075	0.07	0.05	PhA[νCH(99)]
-	3069	3073	0.44	0.06	PhB[νCH(99)]
-	3069	3073	0.21	0.01	PhA[νCH(98)]
3044	-	3057	1.69	0.05	Py[νCH(99)]
-	3036	3035	2.92	0.05	Py[νCH(99)]
1666	1679	1666	100.00	0.12	νC=O(60)
1591	-	1593	18.98	0.62	PhB[νCC(62)] + PhB[δCH(11)]
-	1586	1583	6.59	0.03	Py[νCC(51)] + Py[νCN(16)]
-	-	1571	0.19	1.31	PhA[νCC(60)] + PhA[δCH(15)] + νNN(10) + PhA_{asyd}(10)
-	-	1562	8.12	0.72	PhA[νCC(50)]
-	-	1561	13.87	0.23	Py[νCC(39)] + Py[νCN(23)] + Py[δCH(13)]
-	1542	1542	11.16	0.33	PhB[νCC(50)] + PhA[νCC(11)] + COH[δOH(10)]
1487	1490	1490	35.45	18.72	νNN(42) + PhB[νCC(14)] + PhA[νCC(13)]
1457	1449	1450	9.11	0.02	Py[δCH(41)] + Py[νCC(19)] + Py[νCN(19)] + NH_{roc}(10)
-	-	1445	12.82	1.05	PhB[νCC(26)] + PhB[δCH(23)] + COH[νCO(14)] + PhA[δCH(10)]
-	-	1429	3.26	0.68	PhA[δCH(32)] +

Experimental (cm^{-1})		Calculated {B3LYP/6-311G(d, p)}			
υ_{IR}	υ_{Raman}	υ_{Scaled} (cm^{-1})	IR intensity (%)	Raman intensity (%)	Assignment (% PED, internal coordinates having contribution ≥10% are shown)
					PhA[νCC(19)] + PhB[νCC(18)]
-	-	1421	14.95	9.63	PhB[νCC(26)] + νNN(14) + PhA[δCH(12)] + PhA[νCC(10)]
1413	-	1412	20.10	0.05	Py[δCH(47)] + Py[νCC(30)] + Py[νCN(13)]
-	1397	1396	45.75	0.77	COOH[νCO(27)] + COOH[νCC(21)] + CO_{ipb}(18)
-	-	1379	10.37	5.90	PhA[νCC(46)] + PhA[δCH(23)]
1357	1360	1358	34.75	0.06	SO_{2ips}(52), NH_{roc}(23)
-	-	1341	38.29	1.80	PhB[νCC(56)] + COH[δOH(21)]
1317	1310	1314	6.51	0.04	Py[δCH(41)] + SO_{2ips}(29) + NH_{roc}(19)
-	1297	1297	3.70	0.18	COH[νCO(26)] + PhB[δCH(22)] + PhB[νCC(19)] + COH[δOH(10)]
1281	1272	1275	3.56	0.30	PhA[νCC(75)]
-	-	1255	17.21	0.17	PhB[νCC(47)]
1252	1250	1255	1.72	0.01	Py[νCN(35)] + Py[νCC(32)] + Py[δCH(16)]
-	-	1248	4.58	0.23	PhA[δCH(56)] + PhA[νCC(10)]
-	-	1242	15.27	0.29	Py[δCH(22)] + PhA[δCH(15)] + Py[νCC(14)] + NH_{ips}(10)
1232	-	1233	3.03	0.30	νNC(23) + PhB[δCH(19)] + PhA[νCC(15)] + PhB_{trid}(11)
-	1206	1201	3.13	0.14	Py[νCN(29)] + Py[νCC(27)] + Py[δCH(13)] + NH_{roc}(10)

Experimental (cm^{-1})		Calculated {B3LYP/6-311G(d, p)}			
υ_{IR}	υ_{Raman}	υ_{Scaled} (cm^{-1})	IR intensity (%)	Raman intensity (%)	Assignment (% PED, internal coordinates having contribution ≥10% are shown)
-	1173	1181	2.10	7.05	νCN(24) + PhB[δCH(20)] + PhB[νCC(12)] + PhA[δCH(12)] + PhA[νCC(11)]
1158	1152	1161	40.37	2.90	COOH[δOH(29)] + PhB[νCC(17)] + COOH[νCO(12)]
1148	-	1144	42.38	3.22	COOH[δOH(22)] + PhB[δCH(17)] + COOH[νCO(15)]
1132	-	1124	31.89	0.05	SO_{2ss}(54) + Py[δCH(23)]
1115	1119	1116	4.01	5.35	Py[δCH(36)] + PhA[δCH(25)]
-	-	1111	30.88	8.51	SO_{2ss}(25) + PhA[δCH(22)] + Py[δCH(19)]
1101	-	1099	3.55	0.04	PhB[δCH(68)] + PhB[νCC(16)]
-	-	1078	1.93	0.03	Py[δCH(52)] + Py[νCC(26)]
1078	1079	1074	1.56	0.03	PhA[δCH(72)] + PhA[νCC(22)]
1050	1048	1052	4.82	1.10	PhB[δCH(26)] + PhB[νCC(23)] + PhB_{trid}(17)
-	-	1038	8.41	1.72	PhA[νCC(52)] + νSC(15) + PhA[δCH(14)]
1008	-	1035	1.2	0.07	Py[νCC(64)] + Py[δCH(27)]
-	-	999	0.00	0.00	PhB[gCH(88)]
-	-	992	0.02	0.01	PhA[gCH(89)]
-	-	988	0.23	0.01	Py[gCH(89)]
988	-	986	0.93	0.87	PhA_{trid}(58) + PhA[νCC(27)] + PhA[δCH(10)]
-	-	974	1.12	0.16	Py_{trid}(58) + Py[νCN(21)] + Py[νCC(18)]
-	-	966	0.23	0.00	PhA[gCH(82)] + PhA_{puck}(11)

Experimental (cm^{-1})		Calculated {B3LYP/6-311G(d, p)}			
υ_{IR}	υ_{Raman}	υ_{Scaled} (cm^{-1})	IR intensity (%)	Raman intensity (%)	Assignment (% PED, internal coordinates having contribution ≥10% are shown)
-	-	964	0.30	0.01	Py[gCH(88)]
-	-	930	1.41	0.00	PhB[gCH(76)] + PhB_{puck}(11)
921	-	928	0.66	0.04	PhB[νCC(42)] + νNC(10)
-	-	893	4.10	0.02	Py[gCH(89)]
865	-	868	24.06	0.63	NH_{ips}(41)
-	-	858	1.19	0.23	PhA[νCC(20)] + δNN2(15)] + δNN1(13) + νCN(11)
849	-	846	8.04	0.02	PhB[gCH(44)] + PhA[gCH(24)]
-	-	841	0.29	0.01	PhA[gCH(51)] + PhB[gCH(23)]
-	-	840	0.03	0.02	PhA[gCH(94)]
-	-	816	12.14	0.00	COOH[gCO(40)] + COOH[gCC(18)] + τCOH(17)
805	805	798	4.11	0.09	PhB_{trid}(31) + PhB[νCC(17)] + COH[νCO(13)]
-	-	793	6.35	0.24	δCNS(20) + Py[gCH(14)] + NH_{ss}(13) + Py[νCC(12)]
767	-	771	10.63	0.08	Py[gCH(67)] + Py[gCN(11)]
	-	766	8.37	0.01	τCOH(74) + COOH[gCO(13)]
746	-	748	1.95	0.23	PhB[νCC(23)] + PhA_{asyd}(13) + COOH[νCC(10)]
-	-	726	0.37	0.01	Py_{puck}(62) + Py[gCN(18)] + Py[gCH(17)]
-	710	711	0.32	0.01	PhB_{puck}(51) + COH[gCO(23)]
-	-	683	2.78	0.08	PhA_{puck}(50) + gCN2(11) + PhA[gCH(10)]
683	-	679	6.15	0.07	PhA_{puck}(34) + PhA_{asyd}(10)
656	-	648	19.15	0.10	CO_{ipb}(29) + PhB_{asydo}(14)

Experimental (cm^{-1})		Calculated {B3LYP/6-311G(d, p)}			
υ_{IR}	υ_{Raman}	υ_{Scaled} (cm^{-1})	IR intensity (%)	Raman intensity (%)	Assignment (% PED, internal coordinates having contribution ≥10% are shown)
626	-	636	2.92	0.14	$Py_{asydo}(39) + Py_{asyd}(33)$
-	-	623	3.13	0.10	$PhA_{asydo}(36) + Py_{asyd}(14)$
-	-	618	14.25	0.63	$Py_{asyd}(27) + PhA_{asydo}(16) + \delta CNS(10)$
591	-	589	68.01	0.61	$SO_{2wag}(26) + gNH(12)$
581	-	582	19.45	0.06	$\tau COOH(49) + gNC(12)$
-	-	564	0.95	0.01	gNH(14)
-	-	551	2.33	0.10	$PhB_{asydo}(11)$
549	-	547	0.80	0.02	$gNC(16) + COH[gCO(16)] + PhB_{asyt}(15)$
526	-	532	11.62	0.41	$SO_{2wag}(22)$
-	-	511	3.59	0.06	$SO_{2sci}(13) + Py_{asyto}(13) + Py[gCN(12)]$
509	-	508	9.64	0.11	$Py_{asyto}(18) + Py[gCN(14)] + SO_{2sci}(12)$
-	-	486	4.18	0.18	$COH[\delta CO(24)] + COOH[\delta CO(23)] + COOH[\delta CC(10)]$
-	-	473	1.82	0.11	$PhA_{asyt}(15) + gCN(14) + PhA_{puck}(14) + PhB_{puck}(10)$
456	-	456	2.23	0.01	$PhB_{asyto}(56) + COOH[gCC(20)]$
-	-	436	0.00	0.01	$PhA_{asyto}(78) + PhA[gCH(15)]$
-	-	425	0.01	0.18	$COipb(21) + COH[\delta CO(19)] + COOH[\delta CO(18)] + PhB_{asyd}(14)$
-	-	397	0.20	0.06	$SO_{2roc}(20)$
-	-	387	0.31	0.04	$Py_{asyt}(34) + Py[gCH(10)]$
-	-	384	0.24	0.08	$Py_{asyt}(36) + PhB_{puck}(11) + Py[gCH(10)]$
-	-	359	0.82	0.09	$PhB_{puck}(10)$
-	-	354	1.98	0.02	$COH[\delta CO(19)] + PhB_{asydo}(14)$
-	-	331	1.80	0.07	$\nu SC(21) + SO_{2sci}(10)$

Experimental (cm^{-1})		Calculated {B3LYP/6-311G(d, p)}			
υ_{IR}	υ_{Raman}	υ_{Scaled} (cm^{-1})	IR intensity (%)	Raman intensity (%)	Assignment (% PED, internal coordinates having contribution ≥10% are shown)
-	-	306	0.04	0.12	$NH_{ss}(21) + SO_{2sci}(15)$ + Py[δCN(13)]
-	-	294	0.63	0.04	$\nu SC(11) + SO_{2roc}(10)$
-	-	269	0.28	0.08	$SO_{2twi}(55)$
-	-	256	0.48	0.16	$PhA_{asyt}(19) + Py_{asyto}(17)$ + $SNC_{sci}(11)$
-	-	218	0.01	0.00	COOH[gCC(38)] + $PhB_{asyt}(21)$ + τNC(13)
-	207	198	0.94	0.15	COOH[δCC(31)] + δSC(15)
-	-	192	0.31	0.11	$PhA_{asyt}(19) + Py_{asyto}(17)$ + $SNC_{sci}(13)$
-	-	153	0.18	0.16	$PhA_{asyd}(14)$ + νSC(13)
-	-	139	0.96	0.06	δCNS(40) + τNH(12) + τNS(11)
-	-	137	0.17	0.13	$PhB_{asyt}(37)$ + τCOH(29)
-	-	134	0.13	0.43	δSC(35)
-	103	114	0.08	0.66	gSC(20) + $SNC_{sci}(17)$
-	84	93	0.22	0.16	τPhB(60)
-	68	62	0.03	0.60	$PhB_{asyt}(26)$ + τPhB(15)
-	-	45	0.15	3.64	τSC(26) + τNH(21)
-	-	39	0.03	2.69	δNN1(22) + τSC(19) + δNN2(19)
-	-	33	0.11	3.51	τNH(30) + gNH(23)
-	-	29	0.07	12.48	τNS(34) + τSC(18)
-	-	16	0.05	59.27	gNH(17) + gSC(14)
-	-	9	0.04	100.00	τCN(39) + τSC(18) + τNC(16)

Py, pyridine ring; Ph, phenyl ring (A, B); ν, stretching; δ, bending; τ, torsion; g, gauche; ss, symmetric stretching; ips, in plane stretching; ops, out of plane stretching; sd, symmetric deformation; ipb, in plane bending; opb, out of plane bending; ipr, in plane rocking; opr, out of plane rocking; puck, puckering; trid, trigonal deformation; asyd, asymmetric deformation; asydo, out of plane asymmetric deformation; asyt, asymmetric torsion; asyto, out of plane asymmetric torsion; sci, scissoring; roc, rocking; twi, twisting; wag, wagging.

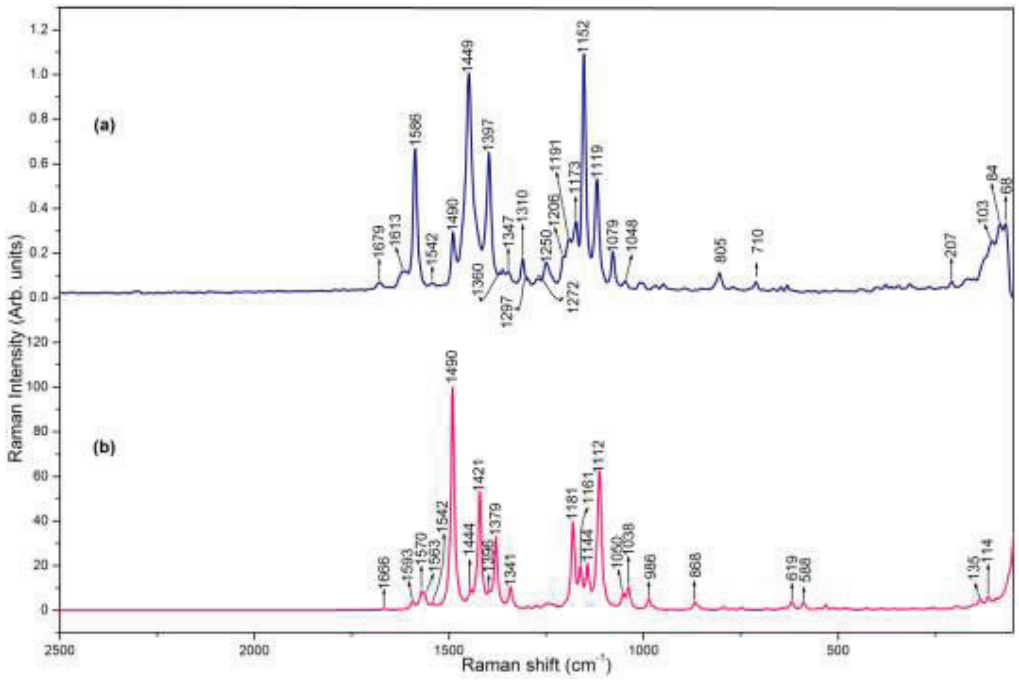

Fig. 5.6 (a) Experimental and (b) simulated Raman spectra of sulfasalazine (2500-50 cm^{-1} region).

5.5 Harmonic oscillator model of aromaticity (HOMA)

Harmonic oscillator model of aromaticity (HOMA) is the structural descriptor of aromaticity. The aromaticity values of pyridine and phenyl rings of sulfasalazine monomer and dimer are presented in Table 5.10. From the tabulated data it is clear that the hydrogen bonding disturbs the aromaticity values. The carboxylic group involved in hydrogen bonding is attached to the Ph B and the Py ring is involved in hydrogen bonding, the aromaticity of Py and Ph B is decreased upon dimerization and aromaticity of Ph A remain unaffected. This is evident from the NBO analysis that the electron density of lone pair nitrogen [$n_1(N_1)$] decreases (~0.058e) and [$\sigma^*(O_{80}–H_{81})$] increases (~0.085e) upon dimerization. The charge is transferred from the Py ring of first molecule to the second molecule thus reducing the aromaticity of pyridine ring.

Table 5.10 Aromaticity values of pyridine and phenyl rings in sulfasalazine.

Ring	HOMA		ΔHOMA
	Monomer	Dimer	
Pyridine (Py)	0.991	0.988	0.003
Phenyl A (Ph A)	0.977	0.977	0.000
Phenyl B (Ph B)	0.901	0.898	0.003

5.6 Conclusion

The molecular structure of sulfasalazine monomer and dimer is modeled using density functional theory with 6-311G (d, p) basis set. The charge transfer arising due to hydrogen bonding is explained by NBO analysis and the strength of hydrogen bond is in the order $O-H\cdots N > O-H\cdots O > N-H\cdots O$. The complete vibrational assignments of the title compound are made by normal coordinate analysis. The shift in the peaks of the hydrogen bond stretching frequency and the corresponding bond length elongation is analyzed. The intermolecular N–H···O, O–H···N and intramolecular O–H···O hydrogen bonds have been investigated. The antibacterial drug sulfasalazine is very stable because of these strong hydrogen bonds and it is broken down into sulfapyridine and 5-ASA in the colon by bacterial enzymes. The aromaticity of the rings (Py and Ph B) involved in hydrogen bonding decreases upon dimerization.